Research of Basic Plasma Physics Toward Nuclear Fusion in LHD

Akio KOMORI and LHD experiment group
National Institute for Fusion Science, Toki, Gifu 509-5292, Japan

(Received 4 January 2010 / Accepted 15 February 2010)

There are various physics issues which the LHD can explore in the research field of transport studies in high temperature plasmas, research for MHD stability in high density and high beta plasma, that are crucial for a future device aimed at nuclear fusion. Physics of the confinement improved mode is discussed with a new paradigm of non-linearity, non-diffusivity and non-locality of the transport. Various MHD modes are observed such as the interchange mode and high energy particle driven modes. Magnetic island physics are intensively studied by applying a perturbation field or by controlling the magnetic shear with NBCD. The LHD also gives opportunities to extend research beyond plasma physics. Research concerning atomic processes such as a test of the collisional-radiative model and energy levels of highly charged heavy ions are also investigated using the plasma in LHD.

Keywords: Large Helical Device, transport, MHD stability, atomic process

DOI: 10.1585/pfr.5.S2001

1. Introduction

The plasma parameters in the Large Helical Device (LHD) have been extended to high density (electron density, $n_e(0) = 1.2\times10^{21}$ m^{-3}) or high temperature (central ion temperature of 5.6 keV at $n_e(0) = 1.6 \times 10^{19}$ m^{-3}, central electron temperature of 10 keV at $n_e(0) = 5.0 \times 10^{18}$ m^{-3}) or high beta ($\beta = 5.1\%$). Because of the wide range of plasma parameters, there are various physics issues which the LHD can explore in the research field of transport studies in high temperature plasmas, research for MHD stability in high density and high beta plasmas, that are crucial for a future device aimed at nuclear fusion.

Figure 1 shows the research fields covered by the experiments in LHD. Steady-state operation and high density experiments are unique features in helical plasmas. The steady state operation is much easier in a helical plasma where the magnetic field is mainly determined by the external coils. This is in contrast to tokamaks where the magnetic field is determined by the plasma current and the strong coupling between the plasma current and transport requires a sophisticated feedback system to keep the steady-sate high performance plasma. The density limit in a helical plasma is mainly determined by the power balance between the heating power and radiation power, while the density limit in tokamak is determined by the Greenwald limit and a high magnetic field ($B \sim 9$ T) is necessary to achieve a high density of $n_e(0) = 1.5 \sim 2\times10^{21}$ m^{-3} [1]. In LHD, a high density plasma can be obtained even at the lower magnetic field of ($B \sim 3$ T) because of no Greenwald limit in helical plasmas.

In this paper, the physics issues which have a linkage to the physics in tokamaks and other fields such as atomic processes and astrophysics are emphasized rather than the physics issue related to the plasma performance which can be extrapolated to a helical reactor because they have been reported elsewhere. Since the transport in LHD is mainly determined by the turbulent transport, except for the case where the neoclassical transport becomes as large as the turbulent transport, the research of transport in LHD would contribute to the understanding of turbulent transport in tokamaks. There are similarities and differences in ITBs between LHD and tokamaks and the experimental study for investigating the mechanism which causes the differences gives a deeper understanding of transport which is necessary for better ITB control in tokamaks. The study of spontaneous rotation due to the non-diffusive term of momentum transport in helical plasma also gives us further understanding of spontaneous rotation in tokamaks which is also indispensable for resistive wall mode (RWM) control. The stochastization of the magnetic field is also important physics for the ELM control in tokamak. The other

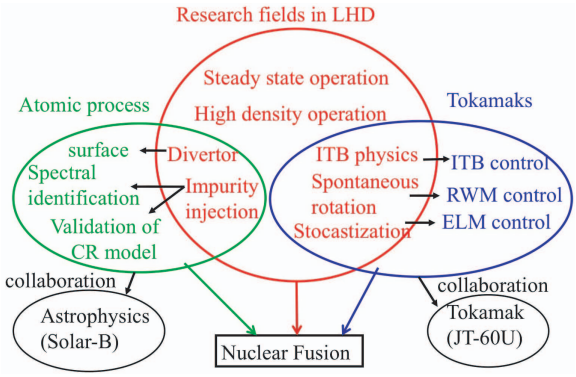

Fig. 1 Research field covered by the experiments in LHD.

author's e-mail: komori@lhd.nifs.ac.jp

aspect of the research in LHD is a link to atomic processes. The experimental study of the edge physics including divertor physics in LHD can contribute the spectral identification and validation of the collisional radiative model (CR model), which is important in the astrophysics, especially in the spectral analysis of the solar atmosphere.

2. Transport

Physics of the confinement improved mode is discussed with a new paradigm of non-linearity, non-diffusivity and non-locality of the transport. Transport in the magnetically confined plasma are complicated because of the non-linearity, non-locality and non-diffusive terms of transport. The non-diffusive terms are attribute to the inter-linkage between particle momentum and radial heat fluxes. For example, the radial fluxes of particle, momentum have diffusive terms, in which the radial fluxes are proportional to the gradients of density, momentum, and non-diffusive terms as offsets of radial fluxes determined by the temperature gradient, which are categorized as off-diagonal terms of the transport matrix.

2.1 Formation of ion internal transport barrier (non-linearity of transport)

High ion temperature plasmas are obtained with a relatively high heating power by both P-NBI and N-NBI with a low electron density of $1 \sim 2 \times 10^{19}\,\mathrm{m}^{-3}$ [2]. It is important to keep the $T_\mathrm{e}/T_\mathrm{i}$ ratio close to or below unity at the onset of the high power NBI to achieve a high ion temperature. There are two approaches to achieve high ion temperature plasmas by keeping the $T_\mathrm{e}/T_\mathrm{i}$ ratio at a low level in LHD. One is to perform the P-NBI injection only before the start of high power heating, which gives a target plasma with a low $T_\mathrm{e}/T_\mathrm{i}$ ratio. The other approach is pellet injection before the start of high power heating, which results in a $T_\mathrm{e}/T_\mathrm{i}$ ratio close to unity. There are two type of pellets: one is a hydrogen fueling pellet and the other is a carbon pellet [3]. The carbon pellet has an additional benefit in increasing the power deposition of NBI to ions through ion-impurity collisions.

Figure 2 shows the normalized ion temperature gradient of R/L_{T_i}, where R is the major radius and L_{T_i} is the scale length of the ion temperature gradient defined as $-(1/a)(\partial T_\mathrm{i}/\partial\rho)$. The normalized ion temperature gradient, R/L_{T_i}, evaluated just inside the foot at $r_\mathrm{eff}/a_{99} = 0.56$, jumps from 7 to 14 associated with the formation of the ion ITB [4, 5]. Here, r_eff is the minor radius averaged with the magnetic flux surface and a_{99} is the effective minor radius in which 99 percent of the plasma kinetic energy is confined and is 0.64 m in this discharge. The time for the transition estimated from the time for the change of the R/L_{T_i} value is 0.1 sec, while the ITB region expands to the inner side gradually (~ 0.2 s). The radial profiles of thermal diffusivity at $t = 2.10$ s (in the L-mode phase), $t = 2.23$ s (just after the formation of the ITB) and $t = 2.33$ s (in the steady-state phase of the ITB) are plotted in Fig. 2 (b). The reduction of the thermal diffusivity is observed in a wide interior region of the plasma (0.19 m $< r_\mathrm{eff} <$ 0.53 m) after the formation of the ITB. The drop of the thermal diffusivity has a maximum at half of the plasma minor radius and the reduction of the thermal diffusivity is by a factor of 2. It also should be noted that the thermal diffusivity even slightly increases outside the ITB region ($r_\mathrm{eff} <$ 0.19 m and $r_\mathrm{eff} >$ 0.53 m) just after the formation of the ITB. Later in the ITB-phase, the ITB region expands towards the plasma center and the reduction of the thermal diffusivity is observed near the plasma center ($r_\mathrm{eff} = 0.1$ m), in the steady-sate phase of the ITB.

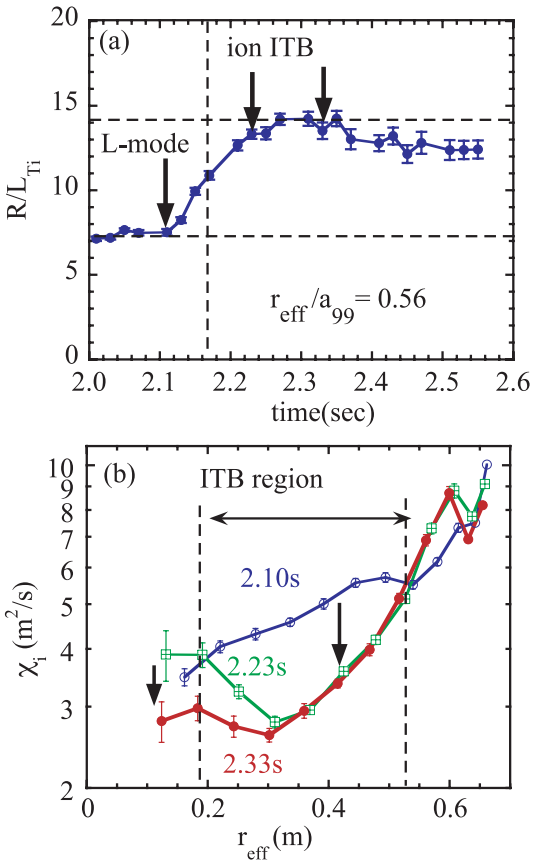

Fig. 2 (a)Time evolution of R/L_{T_i} during the formation of an ITB and (b) radial profiles of ion thermal diffusivity at $t = 2.10$ s (L-mode), $t = 2.23$ s (early phase of ion-ITB) and $t = 2.33$ s (later phase of ion-ITB) in the discharge with carbon pellet injection (from Ref. [4]).

2.2 Core temperature rise by cold pulse (non-locality of transport)

Non-locality of transport is observed in the formation of an internal transport barrier (ITB) as described in the previous section. The ion temperature near the periphery slightly decreases when the central ion temperature increases. The non-locality appears more clearly as a non-local temperature rise, in which the central temperature increases associated with the drop of temperature triggered

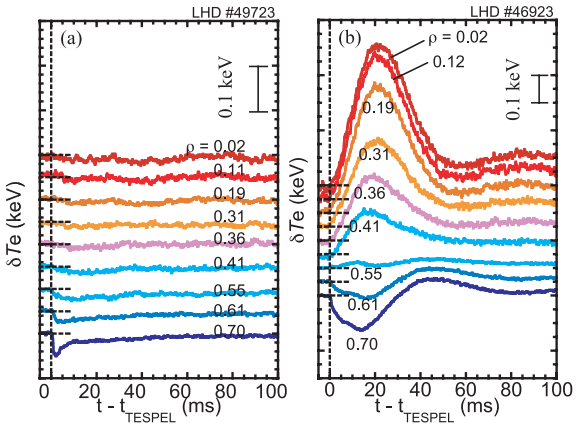

Fig. 3 Time evolutions of the perturbed electron temperature in the plasma with TESPEL injection at (a) high density ($n_e \sim 3.0 \times 10^{19}\,m^{-3}$) and (b) low density ($n_e \sim 0.5 \times 10^{19}\,m^{-3}$) (from Ref [6] modified).

by the tracer-encapsulated solid pellet (TESPEL) injection.

In LHD, the nonlocal core temperature rise is observed in the plasma with relatively low density [6]. Figure 3 shows a typical example of an abrupt increase in core temperature just after the edge cooling. In this example, the diameter of the TESPEL is 420 μm. The plasma is heated continuously by NBI in the co-direction (injected power ~ 2.3 MW) and by ECH (injected power ~ 1.2 MW). As seen in Fig. 3, a non-local core temperature rise is not observed in the plasma with higher electron density, a clear core temperature rise is observed at the lower density with a time scale of 20 ms. The core temperature rise is transit and the core temperature decreases to the previous value associated with the recovery of the edge temperature. The non-local phenomena is sensitive to electron density, which suggests that the turbulence responsible for the space-coupling is enhanced at low density. A similar non-local core temperature rise and collisionality dependence are observed in many tokamaks [7, 8].

2.3 Impurity hole (non-diffusive term of particle transport)

It is well known that the non-diffusive term has a significant contribution to the radial flux of particles and it causes the inward flux which is necessary to achieve a peaked density profile with a particle source localized near the plasma edge. A strong outward convection velocity of impurities is observed in the plasma with an impurity hole, where the impurity density profile becomes extremely hollow after the formation of the ITB [9, 10]. This observation strongly supports the simultaneous achievement of good energy confinement and low impurity concentration, which is necessary for a fusion plasma.

In neoclassical theory, the impurity density profiles are expected to be more peaked than the bulk ions because the density gradient of the impurity should be larger than the density gradient of bulk ions by a factor of the ion

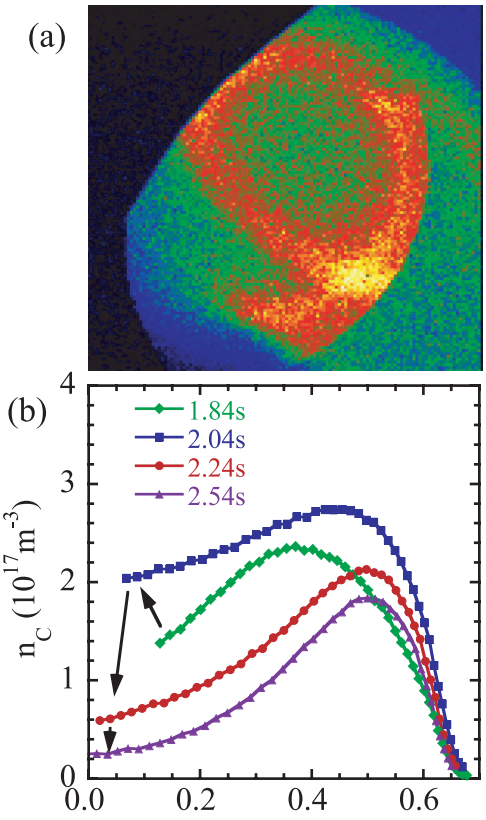

Fig. 4 (a) Soft-X-ray image measured with a tangential X-ray CCD camera after the formation of the impurity hole and (b) radial profiles of carbon density at the L-mode phase (t = 1.84 s), just before the transition from the L-mode to the ITB phase (t = 2.04 s) and at the ITB phase (t = 2.24 s and t = 2.54 s) (from Ref. [10]).

charge Z. This is because both the impurity and bulk ion satisfy the radial force balance and the rotation velocity of the impurity and the bulk ion tend to be equal due to the friction between the impurities and bulk ions. Because the impurity has a higher ion charge, Z, impurity transport is more sensitive to the radial electric field than bulk particle transport. The positive radial electric field in the electron root tends to drive outward flux and suppress the accumulation of impurities and radiation collapse. It is a crucial issue to test the neoclassical prediction in the plasma with an ion-ITB, where the radial electric field is negative and impurity accumulation is expected from neoclassical theory.

Figure 4 shows the soft-X-ray image measured with the soft-X-ray CCD camera with a tangential view after the impurity hole formation. The energy range measured with the soft-X-ray CCD camera is 1-10 keV and K_α lines of Titanium, Iron and Chromium have the dominant contributions. Therefore the soft-X-ray CCD camera is a useful tool to measure the two-dimensional radial distribution of the high-Z impurities. The soft-X-ray image shows the drastic change of the impurity profile from centrally peaked to extremely hollow profiles. The electron density profiles are flat in the L-mode phase and in the

ITB phase, while the profile becomes slightly peaked during the transient phase from the L-mode phase to the ITB phase. The carbon density profile is slightly hollow in the L-mode phase and it becomes extremely hollow in the ITB phase and the central carbon density keeps decreasing and reaches 0.2-0.3% of the electron density at the plasma center. The central carbon concentration is one order of magnitude lower than the carbon concentration near the plasma periphery. The peak of the carbon density is located close to the plasma periphery at $r_{\rm eff} = 0.5$ m and the carbon density gradient becomes positive ($\partial n_{\rm C}/\partial r > 0$) in the plasma core region of $r_{\rm eff} < 0.5$ m , where inward flux due to diffusion is almost balanced by the outward flux due to the strong outward convection velocity. These results clearly show that the impurity hole is observed both in the low-Z impurity (carbon) and in the high-Z impurity when the ion temperature gradient becomes large enough.

2.4 Spontaneous rotation (non-diffusive term of momentum transport)

Spontaneous rotation is one of the important issues in toroidal plasmas, because the plasma rotation is expected to contribute to the suppression of MHD modes, for example the resistive wall mode, which is a serious problem in tokamaks [11–14]. In this plasma, a clear toroidal spontaneous rotation is also observed and rotation driven by the radial electric field is comparable to ones driven by the tangential NBI [15]. These phenomena demonstrate that there are clear non-diffusive terms in the plasma. A spontaneous rotation in the co-direction is observed in the plasmas with an ion internal transport barrier (ITB), where the ion temperature gradient is relatively large ($\partial T_{\rm i}/\partial r \sim 5$ keV/m and $R/L_{T_{\rm i}} \sim 10$) in LHD [16].

Because of the large ion temperature gradients, the magnitude of the spontaneous toroidal flow, $V_\phi^{\rm spon}$, becomes large enough to cancel the toroidal flows driven by tangentially injected neutral beams (NBs) and the net toroidal rotation velocity is almost zero at the outer half of the plasma minor radius even in the plasmas with counter-dominant NB injections. The effect of velocity pinch is excluded even if it exits because of zero rotation velocity. The spontaneous toroidal flow appears in the direction of co-rotation after the formation of the ITB not during or before the ITB formation. The causality between the change in $V_\phi^{\rm spon}$ and $\partial T_{\rm i}/\partial r$ suggests the spontaneous rotation is driven by the ion temperature gradient as the off-diagonal terms of momentum and heat transport. Due to the role of spontaneous toroidal rotation in Magneto-Hydro-Dynamics (MHD) stability, the non-diffusive term of momentum transport has become highlighted in recent momentum transport studies both in helical and tokamak plasmas.

3. MHD Stability

Various MHD modes are observed such as the interchange mode and high energy particle driven modes. Magnetic island physics are intensively studied by applying a perturbation field or by controlling the magnetic shear with NBCD. One of the advantages in LHD is that there are no disruptions, which is typically a problem in a tokamak. A disruption does not take place even though the dynamic response in transport suggests that the magnetic field becomes stochastic in the area of more than one-third of the plasma minor radius.

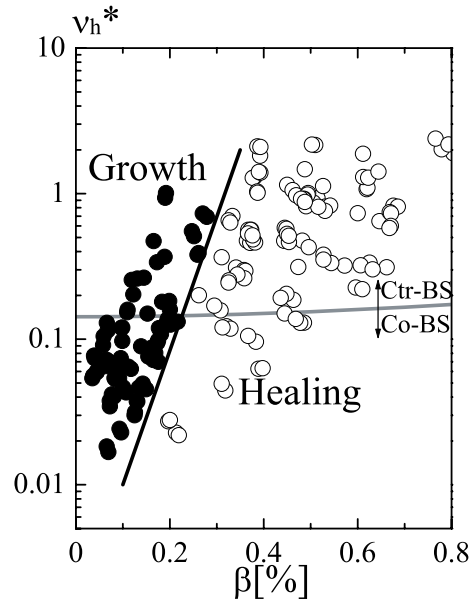

Fig. 5 Growth and healing of magnetic island in the parameter space of beta, β, and normalized collisionality, $\nu_{\rm h}^*$, at the rational surface of $\iota/(2\pi) = 1$ (from Ref. [18]).

3.1 Growth and healing of the magnetic island

The magnetic island appears at the rational surface when the error field exists in the plasma. However, this magnetic island may grow or shrink and disappear depending on the direction of the helical plasma current at the rational surface. The disappearance of the magnetic island due to this current is called "healing" of the magnetic island [17]. It is important to study the mechanism of growth and healing of the magnetic island in order to understand the mechanism for controlling a magnetic island in a toroidal plasma. In the LHD experiment, the magnetic island produced by the perturbation field coils shows a dynamic behaviour depending on beta β and collisionality, $\nu_{\rm h}^*$ [18].

Figure 5 shows the region of the growth and healing of the magnetic island. The magnetic island grows in the lower-β and higher-$\nu_{\rm h}^*$ regime (closed circles) while it disappears in the higher-β and lower-$\nu_{\rm h}^*$ regime (open circles). The boundary indicated by a black solid line can be clearly drawn in the β-$\nu_{\rm h}^*$ space. To investigate the effect of the change of direction of the bootstrap current on the magnetic island, the dependence on the bootstrap current by

the finite beta effect via the change of the magnetic configuration is calculated. The boundary where the bootstrap current reverses is indicated by a grey solid line. The direction is ctr- in the high-ν_h^* regime and co- in the low-ν_h^* regime. It depends on the β, whereas the dependency on the collisionality is weak in the experiment.

3.2 Stochastization of magnetic field at rational surface

Three states of a magnetic island are observed when the magnetic shear at the rational surface is modified using inductive current associated with the neutral beam current drive in the LHD. One state is the healed magnetic island with zero island width. The second state is the saturated magnetic island with a partial flattening of the T_e profile. The third state is characterized by the global flattening of the T_e profile in the core region. As the plasma assumes each of the three states consecutively through a bifurcation process a clear hysteresis in the relation between the size of the magnetic island and the magnetic shear is observed.

Magnetic shear near the plasma core is controlled using inductive current associated with the neutral beam current drive in LHD. This experiment demonstrates that the saturated magnetic island can be healed (no magnetic island) or can be stochastic (large magnetic island) depending on the magnitude of the magnetic shear. There are two bifurcation phenomena observed in this experiment. One is the bifurcation between the saturation and healing of the magnetic island (appearance and disappearance of magnetic island), and the other is a bifurcation between the saturation and stochastization of the magnetic island (appearance and disappearance of stochastization). The stocastization of the magnetic field is observed when the magnetic shear becomes weak. A clear hysteresis in the relation between the size of the stochastic magnetic island and the magnetic shear is observed. This result suggests the importance of the magnetic shear to avoid and eliminate the stochastic magnetic island at the rational surface [19].

3.3 Core density collapse in the high beta plasmas

In LHD the central β can be increased by injecting a hydrogen pellet into the plasma [20]. When the central β exceeds 3% in the standard configuration (magnetic field strength 2.75 T, major radius of magnetic axis of 3.85 m, pitch parameter 1.254 and quadruple field of 100%), the abrupt decrease of central density and pressure are observed as seen in Fig. 6. The central beta is decrease by several tens of percent by this event. The location of the magnetic axis is shifted inward due to the decrease of the plasma β. Then the drop of the electron density in the core is obvious. Though we have named this event "core density collapse (CDC)" due to this characteristic. Since the electron temperature profile is rather flat before the crash, the change in the core electron temperature seems to be small. However, the increase in the electron temperature in the edge region suggest that the core plasma is transferred to the edge region in a convective manner. The ion saturation currents at the divertor plate increase with the crash (delay time is less than 100 μs) [21].

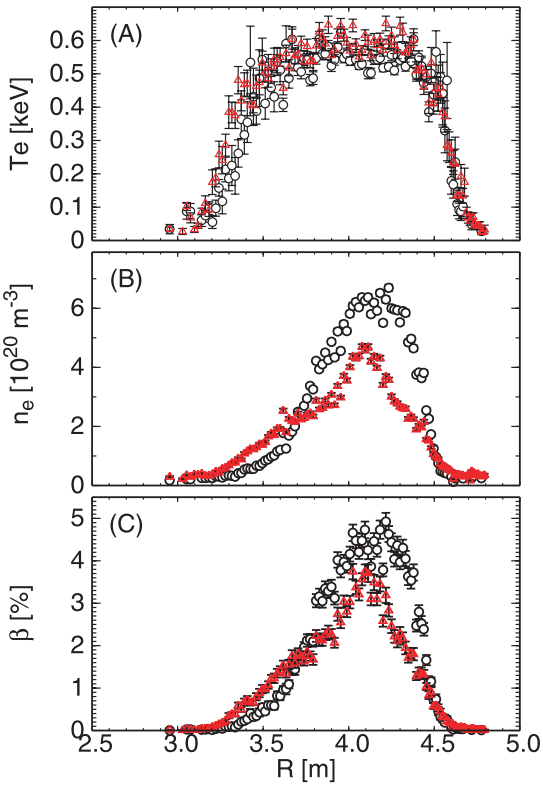

Fig. 6 Radial profiles of (A) electron temperature, (B) electron density and (C) plasma beta before (circles) and after (triangles) the core density collapse (CDC), respectively (from Ref. [21]).

The physics mechanism has been investigated by investigating the relation to the pressure gradient and the local magnetic shear. The stability analysis (estimate of the growth rate of the ballooning mode) by using the stability code Hn-bal [22, 23] suggests that the CDC even is triggered by the high-n ballooning mode near the plasma edge. Since the sign of magnetic shear is opposite to that in a tokamak, this study would contribute to the further understanding of the physics of ballooning modes in toroidal plasma.

3.4 Energetic particle driven MHD instability

In general, energetic ions drive MHD instabilities in helical plasma as well as in tokamaks [24]. Recently, reversed magnetic shear Alfven eigenmodes (RSAEs) having characteristic frequency sweeping were discovered in reversed magnetic shear (RS-) plasmas in tokamaks [25–27]. In LHD, the magnetic shear produced by the external coils are monotonic, however, the reversed magnetic shear can be produced by ctr-NBCD, where the rotational transform at mid-radius decreases by non-inductive current

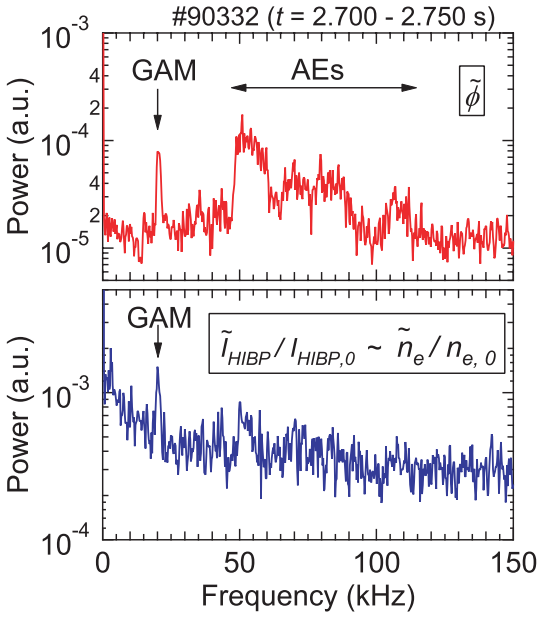

Fig. 7 Frequency spectra of potential and normalized density fluctuation measured with heavy ion beam probe (HIBP) in LHD.

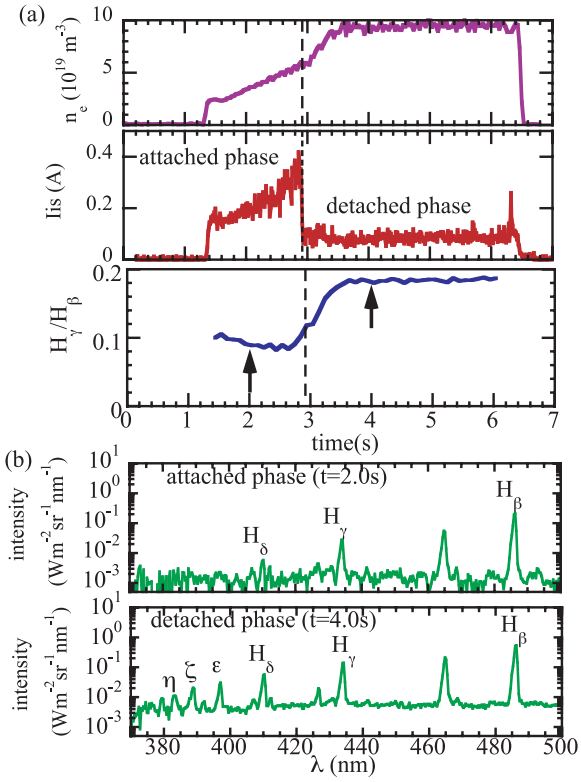

Fig. 8 (a) Time evolution of line-averaged electron density, divertor particle flux at inboard divertor plates (from Ref. [29]) and (b) the ratio of H_γ/H_β and spectra in the ionizing phase (t = 2.0 s) and recombining phase (t = 4.0 s).

and the rotational transform near the plasma center even increases due to the inductive current. In the RS-plasma, the geodesic acoustic mode (GAM) is excited by energetic ions, which is a global type mode different from the localized GAM excited by drift waves.

Figure 7 shows the frequency spectra of the potential and of the normalized density fluctuation measured with heavy ion beam probe (HIBP) in he core region ($r/a \sim$ 0.1-0.4) of plasma with electron cyclotron current drive (ECCD), where weak or reversed magnetic shear is expected [28]. As a coherent mode, the geodesic acoustic modes (GAM) are observed both in the potential and density fluctuations. The potential fluctuations observed in the frequency range of 50-100 kHz are inferred to be Alfven eigenmodes, which are predicted to appear around the local maximum or minimum of the shear Alfven spectra due to the weak or reversed magnetic shear. It is quite interesting to compare the Alfven eigenmodes observed in the plasma with reversed magnetic shear in LHD and tokamaks, where the signs of the magnetic shear itself are opposite (the sign of magnetic shear changes from positive to negative in LHD and negative to positive in tokamak towards the plasma edge).

4. Atomic Processes in the LHD Plasmas

LHD produces excellent profile measurements for density, electron and ion temperature, rotation velocity, radial electric field and rotational transform. Precise profile measurements enable us to study fine plasma physics regarding transport and MHD stability in the high temperature plasmas discussed above. Research concerning atomic processes such as a test of the collisional-radiative model and energy levels of highly charged heavy ions are also investigated using the plasma in LHD.

4.1 Recombining phase in detached plasmas

Because the heat load to the divertor plate in steady-state operation is too large for the efficient heat removal of the current divertor design, it is a crucial issue to reduce the heat load to the divertor plate by increasing the radiation at the plasma periphery. Therefore it is ideal that most of the plasma energy is lost by radiation before the plasma heat flux touches the divertor plate. At low density operation, most of the heat flux is deposited to the divertor plate (attached plasma) [29]. When the density exceeds a critical value, the heat flux to the divertor plate is significantly reduced by the edge radiation, which is called a transition from the attached plasma to the detached plasma. The n/m = 1/1 resonant perturbation field is applied by the coils installed at the top and bottom of the machine in order to create a magnetic island in the stochastic region.

Figure 8 shows the time evolution of the line-averaged electron density, divertor particle flux at the inboard divertor plates and the ratio of H_γ/H_β in the discharge with n/m = 1/1 island. The discharge was initiated by neutral beam injection (NBI) heating at t = 1.3 s, and the density was ramped up by gas puff gradually. The divertor parti-

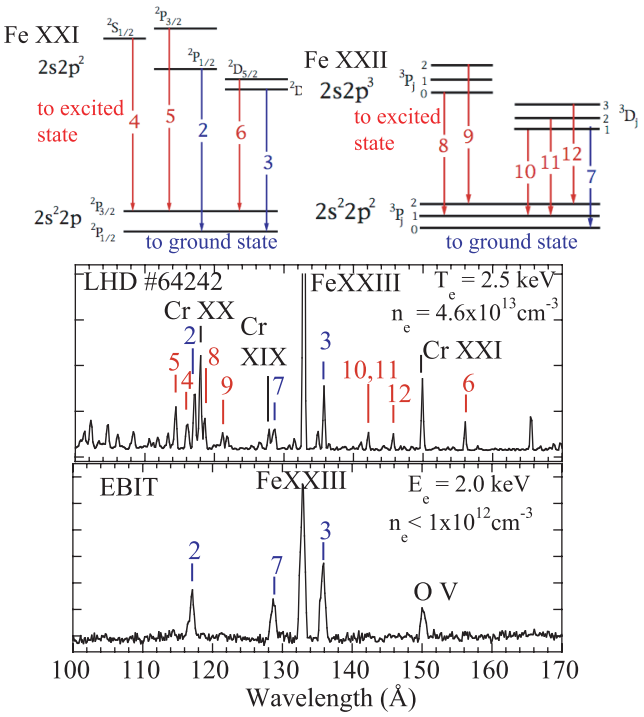

Fig. 9 Energy diagram of FeXXI and FeXXII and spectra observed in the plasma in LHD and in the plasma in an electron beam ion trap (EBIT).

cle flux (ion saturation current) measured by the Langmuir probe arrays increases linearly with respect to the density and the transition from the attached phase to the detached phase takes place at $t = 2.9$ s as indicated with a dotted line. The increase of the intensity ratio of two lines from the Balmer series of the hydrogen atom $H_\gamma(5 \rightarrow 2)/H_\beta(4 \rightarrow 2)$ indicates the transition from the ionizing phase to the recombining phase in the divertor plasma. This transition is more clearly observed in the spectra in Fig. 8 (b). The Balmer lines with higher upper n-level , H_δ, H_ε, H_ζ, H_η, (up to upper level $n_u = 9$) are observed in the recombining phase, while only Balmer lines with lower n-levels (up to $n_u = 6$) are observed in the ionizing phase.

4.2 Transition between excited states in plasmas with impurity injection

Figure 9 shows the energy diagram of FeXXI and FeXXII and spectra observed in the LHD plasma, where an iron pellet is injected, and in an electron beam ion trap (EBIT) [30]. There are significant differences in the spectra observed in an LHD plasma and an EBIT plasma. Only the lines between the excited state and the ground level (lines ♯2, ♯3, ♯7) are observed in the EBIT plasma. This is because the electrons are populated in the ground state in the EBIT plasma. In contrast, there are significant populations in the excited state due to the excitation between the sub-levels $2s^22p$ [$^2P_{3/2}$-$^2P_{1/2}$] and $2s^22p^2$ [$^3P_0$-$^3P_1$-$^3P_2$] because the plasma density is large enough in LHD. This sublevels excitation is due to the electron impact at low temperature < 1 keV and the proton impact at higher temperature of > 1 keV. Therefore the lines between excited states are observed in LHD plasmas. Therefore the spectroscopy using the LHD plasma can contribute to atomic process physics in the identification of spectral lines due to the proton impact excitation, which is difficult in other atomic process experimental devices such as EBIT. It should be also noted that the line emission in LHD plasma is strong enough to give precise measurements (wavelength and intensity of the lines) and as a test for atomic data and the collisional radiative model.

5. Summary

There are various physics issues which LHD can explore in the research field of transport studies in high temperature plasmas, research into MHD stability in high density and high beta plasmas, that are crucial for a future device aimed at nuclear fusion. The non-locality appears as a non-local temperature rise, in which the central temperature increases associated with the drop of temperature triggered by impurity pellet injection. Non-locality is also observed in the formation of an internal transport barrier (ITB). The ion temperature near the periphery slightly decreases when the central ion temperature increases. A strong outward convection velocity of impurities is observed in the plasma with impurity hole, where the impurity density profile becomes extremely hollow after the formation of an ITB. This observation strongly supports the simultaneous achievement of good energy confinement and low impurity concentration, which is necessary for a fusion plasma.

Magnetic island physics are intensively studied by applying a perturbation field or by controlling the magnetic shear with NBCD. Magnetic islands can be healed as the β is increased or collisionality is decreased and the stocastization of the magnetic field is observed when the magnetic shear becomes weak. The collapse of central β is observed in the region of high central β plasma in LHD. In divertor plasmas, the atomic processes become important. The transition from the ionizing phase to the recombination phase are observed associated with the transition from the attached plasma to detached plasma. The impurity pellet injection experiment in LHD gives opportunities to study atomic processes, especially the sub-levels excitation due to plasma.

In conclusion, various physics issues that are related to the comprehensive understanding of toroidal plasma in the topics of turbulent transport, MHD stability, and atomic processes have been performed in LHD by taking advantage of a wide range of plasma parameters.

[1] M. Greenwald *et al.*, Phys. Rev. Lett. **53**, 352 (1984).
[2] M. Yokoyama *et al.*, Phys. Plasmas **15**, 056111 (2008).
[3] S. Morita *et al.*, J. Plasma Fusion Res. **79**, 641 (2003).
[4] K. Ida *et al.*, Nucl. Fusion **49**, 095024 (2009).

[5] K. Nagaoka *et al.*, Plasma Fusion Res. **3**, S1013 (2008).
[6] N. Tamura *et al.*, Nucl. Fusion **47**, 449 (2007).
[7] P. Galli *et al.*, Nucl. Fusion **39**, 1355 (1999).
[8] F. Ryter *et al.*, Nucl. Fusion **40**, 1917 (2000).
[9] M. Yoshinuma *et al.*, Nucl. Fusion **49**, 062002 (2009).
[10] K. Ida *et al.*, Phys. Plasmas **16**, 056111 (2009).
[11] K. Ida *et al.*, Phys. Rev. Lett. **74**, 1990 (1995).
[12] J. Rice *et al.*, Nucl. Fusion **38**, 75 (1998).
[13] Y. Sakamoto *et al.*, Nucl. Fusion **41**, 865 (2001).
[14] M. Yoshida *et al.*, Phys. Rev. Lett. **100**, 105002 (2008).
[15] K. Ida *et al.*, Phys. Rev. Lett. **86**, 3040 (2001).
[16] M. Yoshinuma *et al.*, Nucl. Fusion **49**, 075036 (2009).
[17] K. Narihara *et al.*, Phys. Rev. Lett. **87**, 135002 (2001).
[18] Y. Narushima *et al.*, Nucl. Fusion **48**, 075010 (2008).
[19] K. Ida *et al.*, Phys. Rev. Lett. **100**, 045003 (2008).
[20] N. Ohyabu *et al.*, Phys. Rev. Lett. **97**, 55002 (2006).
[21] S. Odachi *et al.*, Contrib. Plasma Phys. **50**, 552 (2010).
[22] N. Nakajima, Phys. Plasmas **3**, 4545 (1996).
[23] N. Nakajima, Phys. Plasmas **3**, 4556 (1996).
[24] K. Toi *et al.*, Plasma Phys. Control. Fusion **46**, S1 (2004).
[25] H. Kimura, *et al.*, Nucl. Fusion **38**, 1303 (1998).
[26] S. E. Sharapov *et al.*, Phys. Lett. A **289**, 127 (2001).
[27] R. Nazikian *et al.*, Phys. Rev. Lett. **91**, 125003 (2003).
[28] T. Ido *et al.*, Plasma Sci. Tech. **11**, 460 (2009).
[29] M. Kobayashi *et al.*, Phys. Plasmas **17**, 056111 (2010).
[30] H. A. Sakaue *et al.*, "Electron density dependence of intensity ratio for FeXXII EUV emission lines arising from different ground levels in Electron Beam Ion Trap and Large Helical Device" submitted to J. Appl. Phys.